Self Phase-Stabilized Heterodyne Vibrational Sum Frequency Generation Microscopy

Haoyuan Wang[1], Tian Gao[1,2], Wei Xiong[1]

[1] Department of Chemistry and Biochemistry, University of California San Diego, La Jolla, CA
[2] College of Chemistry and Molecular Sciences, Wuhan University, Wuhan, PR China

ABSTRACT: Vibrational sum frequency generation (VSFG) spectroscopy has been a powerful technique to probe molecular structures at non-centrosymmetric media. Recent developed heterodyne (HD) detection can further reveal spectral phase and molecular orientations. Adding imaging capability to an HD VSFG signal can bring spatial visualization capability into this non-linear optical technique. However, it has been a challenge to build an HD VSFG microscope that is both easy to align and has good spectral phase stability – two necessary criterions for the broad application of this technique into various areas of science. Here, we report a fully-collinear HD VSFG microscope, which meets both phase stability and optical alignment requirements that can spatially resolve images of molecular interfaces and domains, with chemical and structural sensitivities. The phase stability is more than nine times better than a Michelson Interferometric HD VSFG microscope. Using this HD VSFG microscope, we study the structures of molecular self-assembly films. Because of the superior phase sensitivity, we successfully identify two molecular domains with different molecular orientations, which we show is not possible to extract from an ensemble-averaged VSFG spectrum or homodyne-detected VSFG image.

Keywords: vibrational sum frequency generation, microscopy, phase-resolved, self-assembly, non-linear optics

TOC graphic:

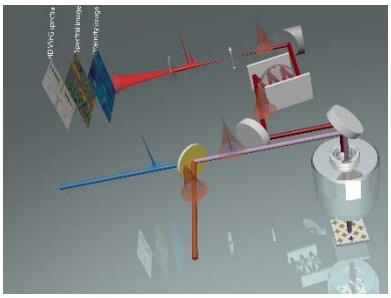

Molecular specific imaging on non-centrosymmetric molecular interfaces and domains[1–12] is crucial for understanding structures and dynamics on many inhomogeneous systems, such as chemical reactions on heterogeneous catalysts,[13] protein interactions with lipid bilayers,[14] structure of optical metamatials,[15] and formation of structure color materials.[16] By spatially resolving interfaces and domains, microscopy could obtain domain specific knowledge and mitigate ensemble averaging.[17–21] Yet, in traditional optical microscopy, signals of non-centrosymmetric molecular interfaces and domains are often overwhelmed by those of isotropic bulk materials. Even-order nonlinear optical microscopy, such as second harmonic generation (SHG) microscopy,[22] has been a popular technique to image non-centrosymmetric systems and is widely implemented in biophysics. However, SHG does not have molecular specificity. An alternative approach is vibrational sum frequency generation (VSFG) microscopy.[5,9–11] A VSFG microscope is ideal to obtain comprehensive knowledge of complex systems: it has chemical sensitivity by probing vibrational signatures and spectral lineshape[23–25] of molecular functional groups; it has symmetry sensitivity similar to SHG to selectively probe areas that are non-centrosymmetric; it also has spatial resolutions to remove ambiguities from the ensemble average of large areas. In addition, heterodyne detection scheme and recent advances in long term stablitities[26–36] enable the measuring of absolute orientations of molecular vibrational modes, which adds structural sensitivity to the microscope. Thus, a heterodyne (HD) VSFG microscope could reveal new, more comprehensive information of molecular interfaces and domains, which is superior to existing imaging techniques.

HD VSFG microscopy is challenging, however, because two ultrashort laser pulses of different colors need to be overlapped spatially and temporally, and the frequency of emitted signal is at the sum of frequencies of these two input pulses.[23–25] The involvement of multiple color pulses imposes many technical challenges when using HD VSFG microscopy, and heterodyne detection is one of the biggest difficulties: experimental techniques such as self-heterodyne,[37,38] which is widely used in pump probe and 2D spectroscopy, cannot be implemented. In order to perform heterodyne detection, a local oscillator (LO) pulse that is at the same frequency as the VSFG signals has to be generated separately and collinearly aligned with the VSFG signals.[39,30,31,33–36] To date, the only reported HD VSFG microscopy used a Michelson Interferometric geometry.[40] In this geometry, LO is generated in one of the Michelson Interferometer arms and combined with VSFG signals in the other arm. Because LO and VSFG signals are generated in two separated beam paths, mechanical stability is extremely important to eliminate any phase drift. Furthermore, an interferometric geometry also presents challenges in alignment and maintenance.

In this article, we present the first fully collinear HD VSFG microscope, which demonstrates excellent phase stability and circumvents technical challenges in spectrometer alignments. To further extract comprehensive molecular knowledge from VSFG images, we developed a spectral pattern recognition code based on a greedy algorithm. Using this code, we can differentiate domains with various molecular conformations, which would otherwise be difficult to distinguish using optical imaging techniques[41] or homodyne VSFG microscopes.[4–12] We implemented this phase-stable collinear HD VSFG microscope to study a guest-host molecular self-assembly[42] spin-coated on gold. We found that the self-assembly contains non-centrosymmetric domains at sizes from about 20 to 100 μm^2, and there are mainly two types of domains, which have opposite molecular alignment relative to each other. This microscope development should pave the way for implementing HD VSFG imaging in a broad range of applications in biophysics,[43] materials[44] and surface sciences.[45,46]

The core experimental setup of HD VSFG microscope is illustrated in Figure 1. A mid-IR pulse is generated by a TOPAS pumped by a Ti:sapphire 30 fs, 800 nm laser, followed by a home-built difference frequency generation (DFG) setup. The residual 800 nm (1.12 mJ) after TOPAS is sent into a 4f geometry pulse shaper to generate a spectrally narrowed upconversion pulse (output energy is 1.2 μJ, FWHM is 3.8 cm^{-1}, and the

pulse shape is Gaussian with a pulse duration of 4 ps). The mode of the upconversion pulse is optimized by passing through a spatial filter. Mid-IR and upconversion pulses are then combined by a customized dichroic optics (Newport), which passes mid-IR and reflects 800 nm lights. After the dichroic optics, both mid-IR and 800 nm pulses are collinear and overlapped temporally, and then they are focused together by a Schwarzchild (Edmund Optics, 15X/0.28NA) reflective objective lens onto samples. The Schwarzchild objective lens is used to circumvent optical aberrations caused by refractive index differences of light at various frequencies. The generated VSFG signals, along with incident mid-IR and upconversion pulses are reflected off a sample and are collected by the same objective lens. Because the incident beams are sent through one side of the objective entrance, the reflected beams are offset relative to incident beams after exiting the objective lens.

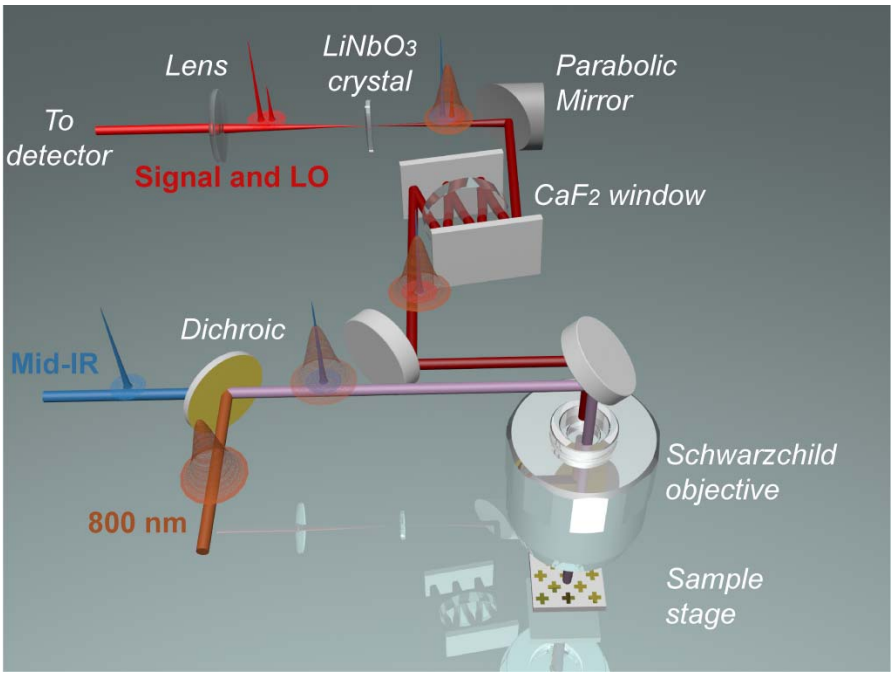

Figure 1 Schematic of the collinear heterodyne SFG microscopy system. Mid-IR and upconversion pulses are combined collinearly and overlapped temporally by a customized dichroic optic. These incident beams are sent through one side of a Schwarzchild objective lens to be focused on the sample. The reflected beams are offset relative to incident beams and picked up by a mirror. After the pick-up mirror, the VSDG signal, mid-IR and upconversion pulses are overlapped spatially and temporally. These three pulses are passed through a CaF_2 window to generate a time delay between VSFG signal and mid-IR and are then focused on a $LiNbO_3$ crystal to generate a local oscillator that is spatially collinear overlapped but temporally delayed relative to the VSFG signal.

The reflected VSFG signal, mid-IR and upconversion pulses are picked up by a mirror, and all three pulses to spatially and temporally overlap with each other. These three pulses are passed through an optical media to create relative time delays between the pulses.[35] The time delay is necessary to ensure interference fringes between LO and SFG signals for heterodyne detection. In our setup, these pulses are bounced between two parallel mirrors and passed through a 7 mm CaF_2 window four times to generate about 2 ps time delay between SFG signal and mid-IR pulse. It is possible to generate the time delay, because there are non-negligible differences between refractive indices of VSFG signal and mid-IR pulse. The upconversion 800 nm pulse has a similar refractive index to a visible pulse, so it is delayed by a similar amount as the SFG signal. The 2 ps time delay is a "sweet spot" for LO generation. Because the pulse duration of upconversion is 4 ps, the mid-IR pulse temporally overlaps with the front tail of the delayed 800 nm upconversion pulse, which ensures LO generation, and creates the largest amount of time delay and therefore more interference

fringes for extracting spectral phases. A one pass through a 3 cm rode would perform the same function. After generating time delays, the beams are focused into a $LiNbO_3$ crystal (MTI Corp., optical grade, X-cut, 10×10×0.5 mm) to create a LO, through an SFG process. Because SFG on the crystal is impulsive, a LO is only generated when mid-IR and upconversion 800 nm pulses overlap temporarily. Thus, LO duplicates the temporal profile of mid-IR and is delayed relative to SFG signal. The LO and SFG signals are then sent through a few bandpass filters to remove any residual upconversion pulses and are focused into a spectrograph and detected on a charged coupled device (CCD) camera. The LO and SFG signals interfere with each other on the camera to generate heterodyned signals - an interference fringe pattern. The fringe space ($\Delta\omega$) and time delay between LO and VSFG signal (t) satisfy the relation $\Delta\omega \cdot t = 1$. Chirps originated from GVD/TOD of CaF_2 is negligible (SI). To obtain an HD VSFG image, the sample is scanned spatially by an automated stage. The exposure time for each pixel is 2 seconds, and for a typical 100 μm×100 μm image, the scanning time is about 2 hours. The heterodyne interference fringes are Fourier transformed into time domain, where an apodizing filter is applied to remove any DC signal.[33,36,47] The time domain data is inverse Fourier transformed back to frequency domain. The frequency domain molecular VSFG spectral phases are calibrated by nonresonance SFG spectra of z-cut quartz,[33] which results in imaginary and real parts of molecular VSFG spectra. We note our current scheme works for Gaussian shape upconversion pulses, but not for Etalon shape pulses, because mid-IR is ahead of upconversion pulses when arriving at $LiNbO_3$ crystal, and therefore cannot overlap with Etalon upconversion pulses. This issue can be solved by generating LO before the sample.[35]

The largest advantage of this new HD VSFG microscope is that a LO pulse is created from the same pulses that generate VSFG signals. The benefits are three-fold: First, LO is intrinsically collinear with the VSFG signal, because they are generated by the same collinear mid-IR and upconversion pulses. This geometry eliminates the necessity of extra procedures to align LO to be collinear with the VSFG signal, which is difficult but also the most critical factor in heterodyne detection. Second, the spectral phase measured using this new setup is not sensitive to sample height. In heterodyne detection, where LO is generated on a different beam path as signals, a small change of sample heights (~ 200 nm) is enough to change the spectral phase. In our setup, because all pulses are reflected from the sample, height variations would change the beam paths of all pulses together. Thus, the measured phase only reveals molecular orientations, but not sample heights. Third, because all beams travel along the same beam path, phase fluctuation and drifts due to mechanical instability are largely alleviated. To illustrate this benefit, we measure the phase of HD VSFG signal as a function of time, acquired using this collinear HD VSFG microscope and a Michelson Interferometric HD VSFG microscope. The Michelson Interferometric HD VSFG microscope (SI Fig. S1) uses the same optical parts as the collinear setup, except that an additional arm is used to generate LO. Thus, each microscope experiences the same amount of mechanical instability. In 12 mins of measurements using the Michaelson Interferometric HD VSFG microscope, the standard deviation of phase is 0.44 radians, with the largest variation being 2.81 radians. Although phase acquired from the Michelson Interferometric setup does not drift over 12 mins of measurements, spectral phase does fluctuate randomly on a large scale in the time frame of 10 s. On the other hand, the collinear HD VSFG microscope demonstrates a rock-solid phase stability, with 0.039 radians standard deviation and 0.35 radians being the largest variation (Fig. 2a). Thus, the collinear setup enhances phase stability by at least nine times. In addition, the collinear HD VSFG microscope shows good long-term phase stability. During a two hour window, the phase only drifted about 0.032 radians. As mentioned above, the image scan time is about 2 hours. Thus, this phase stability is critical for improving the fidelity of phase extracted from point-to-point scanning heterodyne microscope.

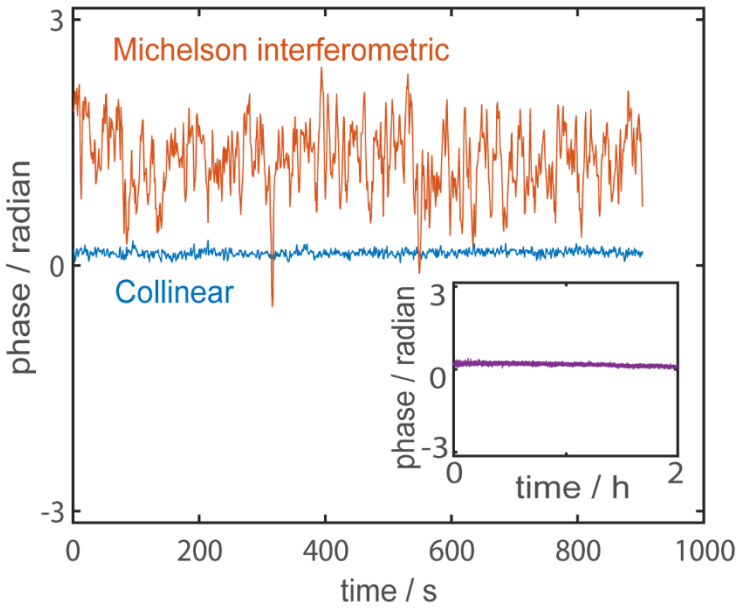

Figure 2. Phase stability of HD VSFG microscope. Collinear HD VSFG microscope shows little phase fluctuations in both short (blue) and long (insert, purple) terms. In comparison, a Michelson interferometric setup shows overall stable phase, but large fluctuations at 10 s time scales.

Next, we examine the quality and resolution of microscopic images. We acquire and compare optical and HD VSFG images of a lithographic pattern composed of gold and GaAs. SFG signals from gold and GaAs form good contrasts, as GaAs has a larger SFG signal than gold. Comparing the two images shows that the SFG image captures all the features shown in the optical image, including edges and the curved corners (Figs. 3a and 3b). To determine the resolution, we scan across sharp edges between gold and GaAs and fit the first order derivative of SFG intensity into a Gaussian model. We found the resolution is < 2 μm, which is close to the theoretical limitation (1.2 μm) defined by the 80% separation criterion[48] (Fig. 3c) . The resolution can be further improved by expanding the 800 nm beam size or using a larger numerical aperture (NA) objective, which is beyond the scope of this report.

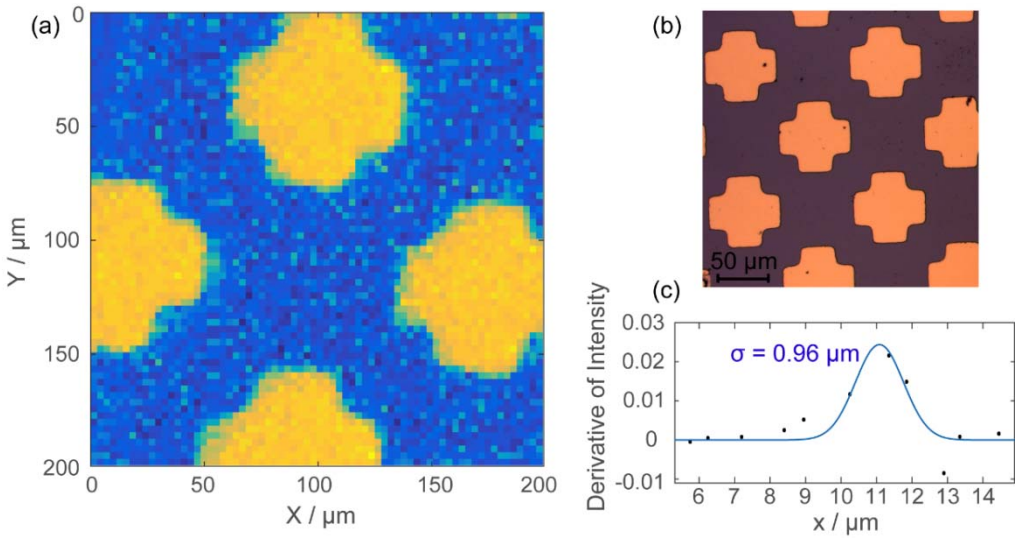

Figure 3. Image and resolution examination of sample pattern. (a) HD VSFG and (b) optical images of a GaAs/Au pattern. (c) Scan across the GaAs/Au edge, Gaussian fitting of the first derivative of SFG intensity. Based on 80% separation criterion, the resolution is about 1.8 μm.

After examining phase stability and resolution, we use the collinear HD VSFG microscope to investigate molecular self-assembly systems spin-coated on gold. The molecular self-assembly is formed by sodium dodecyl sulfate (SDS) and β-cyclodextrin (β-CD) through host-guest interactions, which is a good building-block for responsive molecular devices and bio-mimic structures.[42,49] β-CD forms a cup shape structure, with one of the rim narrower than the other (SI Fig. S2). One SDS molecule can form a complex with two β-CDs, and the conformation of the two β-CD molecules can be head-to-head, tail-to-tail or head-to-tail. Simulations have shown that the head-to-head configuration is the most stable due to more hydrogen bonds.[50] However, head-to-tail conformations can also exist. Most existing techniques cannot distinguish between these different conformations, but the VSFG signal has a unique ability to identify head-to-tail conformations, because head-to-tail conformations are non-centrosymmetric and generate strong VSFG signals.[51] Thus, the HD VSFG microscope is ideal for spatially differentiating between head-to-tail and head-to-head conformations.

The HD VSFG microscope image of molecular self-assembly contains ample spectroscopic information, including spectral intensity, phase, peak position and line shapes (Fig. 4). By plotting the image based on different spectral features, various molecular aspects of these self-assemblies can be obtained. One approach is to plot the absolute integrated VSFG intensity image (Fig. 4e). Based on this intensity image, we conclude the self-assembly sample is very inhomogeneous, composed of domains that have strong and weak VSFG signals, and the size of the domains range from 20 to 100 μm^2. Because molecular self-assembly fully covers gold substrates, the difference in VSFG intensity reflects various domain conformations, but not surface coverage: e.g., domains with strong VSFG signals consist of head-to-tail conformations, because they are non-centrosymmetric, whereas domains with weak signals are composed of head-to-head configurations.[51]

However, there is much more information to be learned than what the VSFG intensity image can reveal, because in the HD VSFG image, each pixel encodes a phase-resolved HD VSFG spectrum. To take advantage of the rich spectral information, we further characterize each domain by comparing all the spectral patterns of their imaginary spectra (corresponding to absorptive spectra),[30,33,34,36,47] including peak position, phase and line shapes. This spectral pattern recognition is done by a greedy algorithm,[52] which

can be easily extended to images that contain large data points. The algorithm sorts every pixel in the image based on its spectral similarity in every run, and iterates the comparing mechanism until the sorting results converge. Then, pixels that are grouped as the same type are plotted in the image with the same color.

Using the spectral pattern recognition code, HD VSFG images of molecular self-assembly are sorted based on spectral similarity. We found six types of spectra in the image, with type 1 and 2 dominating (green and orange in Figs.4a, and 4d). The HD VSFG image is replotted as a spectral image, in which pixels of the same spectral type are coded with the same color (Fig. 4a). The spectral image shows that pixels within each domain have the same spectral type, which indicates molecules in each domain adopt the same conformation. This result agrees with VSFG signal selection rules: VSFG can only survive when the interfaces or domain formed by molecules are ordered and non-centrosymmetric. Otherwise, their signals cancel each other out.[23–25] We note that there are four minor spectral shapes in the HD SFG image (bottom four of Fig. 4c). These minor spectral pixels often appear at the edges or boundary of a domain. Thus, we assume these spectra to be signatures of domain edges, whose structures are not as ordered as those of molecules at the centers of domains, or they are signatures of boundaries between two domains with different conformations, whose spectra should be an average result of molecules in both domains.

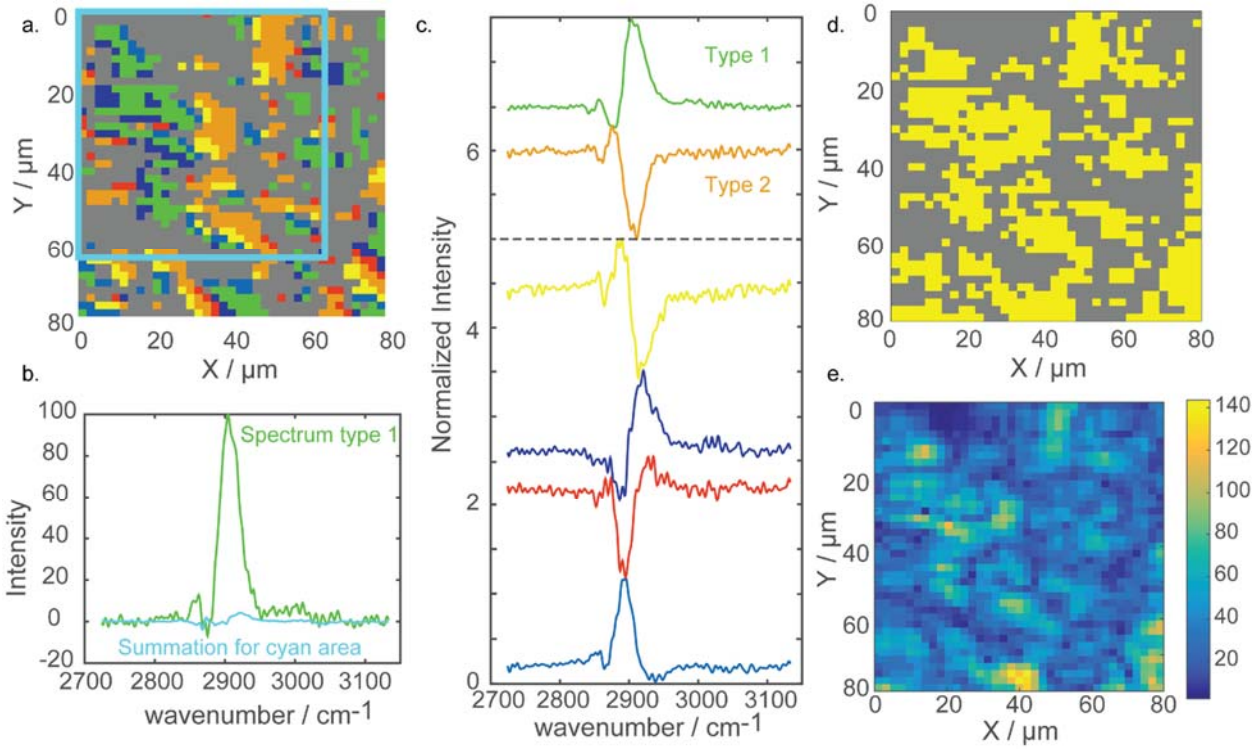

Figure 4. HD SFG image of molecular self-assembly. (a) Domain assignment of HD SFG image by the spectral pattern recognition code: pixels with similar spectral line shape are coded to the same color. (b) Summation of the cyan area (60 μm × 60 μm) in (a) mimics an ensemble-averaged HD SFG imaginary spectrum. It shows that under ensemble-average, HD SFG signals are mostly cancelled out. (c) Color coded HD SFG imaginary spectra that corresponds to the same colored pixels in (a). Type 1 and type 2 are imaginary spectra of two dominant types and the rest of four are spectra of minority pixels at boundary of domains (d) Domain assignment of the absolute square of HD SFG signal (equivalent to homodyne SFG), which shows phase is critical information for spectral recognition. (e) The HD SFG intensity image, which reveals various domains existing at the surface, but is lacking molecular information.

The two dominating imaginary spectra have features that are similar to each other, but are out of phase by π (top two of Fig. 4c). Both spectra include two noticeable peaks, a large peak at 2900 cm^{-1} and a small peak at 2870 cm^{-1}. A control experiment to measure the VSFG signal of deuterated SDS/β-CD molecular

self-assembly shows that the VSFG spectral phase of deuterated SDS/β-CD is similar to the non-deuterated complex (SI Fig. S3). Because deuteration shifts the CH stretch of SDS to 2000 cm^{-1},[53] this result suggests the two vibrational peaks of Fig. 4c originate mainly from β-CD. This conclusion agrees with a previous study on a similar molecule.[54] Based on literature reports, we assign the peak at 2900 cm^{-1} to be the asymmetric modes of CH_2 in β-CD, and the peak at 2870 cm^{-1} to be the CH stretch of β-CD.[54] There are no CH_3 peaks of SDS observed because of the relatively small population of CH_3 groups in molecular self-assemblies.

From peak assignments and corresponding spectral phases, we can determine molecular orientation in each domain. As discussed previously, the molecules in domains that are visualized in HD VSFG microscopy should correspond to the head-to-tail configuration, which generates strong VSFG signals. Based on Gaussian calculation,[55] the vibrational transition dipole vector of CH asymmetric modes are rigid and always point from narrow to wide rims of the β-CD cup. Thus, we conclude that domains with type 1 spectra correspond to self-assembly aligned with the cup facing down, and molecular self-assembly in domains with type 2 spectra faces opposite directions. (Fig.,4d) The CH_2 asymmetric mode highly depends on local hydrogen-bond environments, and its orientation relies on whether the basis-sets and methods used in calculation can properly model hydrogen bonding[56], which is out of the scope of this work. However, because the CH_2 peak always has an opposite sign to the CH peak, it indicates the CH_2 asymmetric mode has stable orientations due to hydrogen-bonding networks, and always points in the opposite direction of CH vibrational mode. More detailed structure study of the molecular self-assembly will be reported in the future.

The ability to distinguish domains in HD VSFG microscopy is not possible with heterodyne VSFG spectroscopy or homodyne VSFG microscopy. First, to show the difference between HD and homodyne VSFG microscope images, we calculate the homodyne VSFG spectra by taking the absolute square of HD VSFG spectra.[33,34,36,47] Then, we use the same spectral pattern recognition code to analyze this homodyne VSFG image. We found all domains are sorted into the same type (Fig. 4d), because the phase information is lost in homodyne signals. Second, to see how spectra of this self-assembly would look like in an HD VSFG spectrometer that measures areas with diameters of 50 to 100 μm, we sum all heterodyne VSFG spectra inside of the cyan squared area (60 x 60 μm^2). The summed spectrum (cyan) in Fig. 4b appears to have a negligible spectral intensity compared to a VSFG spectrum from a single pixel in the HD VSFG image (Fig. 4a). This is because spectra with different phases destructively interfere with each other in the cyan square. If the ensemble-averaged HD SFG spectrum is used to study structure of this self-assembly, a conclusion that no head-to-tail self-assembly exists in this sample could be made, but would be misleading. Thus, the HD VSFG microscope is an essential tool to reveal spatial inhomogeneity, deconvolve ensemble-averaged spectra and resolve spectral phase to determine molecular conformations.

In conclusion, we report a new design of HD VSFG microscope that shows a nine-fold improvement in phase stability. This increase in stability greatly enhances the fidelity of spectral phase extracted from the scanning microscope. In addition, LO is intrinsically collinearly aligned with the VSFG signal, which ensures a heterodyne signal of excellent quality and makes spectrometer alignment simple. To further take advantage of the richness of VSFG spectral information, we implemented a spectral pattern recognition code. We used the microscope and code to investigate molecule self-assembly samples, and identified two molecular domains with opposite molecular orientation. The simplicity of alignments and stability of spectral phase of this new HD VSFG microscope lay the technical foundation for unraveling comprehensive molecular spectral knowledge and opening new avenues for studying in-depth molecular physics of molecular interfaces and domains in environmental surfaces,[57,58] heterojunction materials,[59] biological systems,[14,43] and surface catalysts.[13,44] The design can also be modified and developed into a wide field

illuminated HD-VSFG microscope in combination with compressive sensing to increase data acquisition speed.[60]

EXPERIMENTAL SECTION

Preparation of molecular self-assembly. The sodium dodecyl sulfate (SDS) and β-cyclodextrin(β-CD) were purchased from Sigma-Aldrich. SDS was recrystallized for three times and surface tension curve was measured to check purities.[61] β-CD was recrystallized and kept in a vacuum oven overnight to remove residual water. To prepare molecular self-assembly, SDS and β-CD were mixed at a mole ratio of 1:2, respectively. A suspension of SDS and β-CD was made, with the total concentration being 10 wt%. The suspension was heated until it transformed into a transparent solution and then kept at room temperature for at least 48 hours to self-assemble. The molecular self-assembly was spin-coated onto gold slides at a spin speed of 3000 rpm for 2 mins.

ASSOCIATED CONTENT

Supporting Information

AUTHOR INFORMATION

Corresponding Author

*E-mail: w2xiong@ucsd.edu

ORCID

Wei Xiong: 0000-0002-7702-0187

Haoyuan Wang: 0000-0002-6226-6328

Notes

The authors declare no competing financial interest

ACKNOWLEDGMENTS

This work is supported by the Defense Advanced Research Projects Agency (DAPRA), D15AP000107. Haoyuan Wang is supported by the National Science Foundation (NSF) through the Centers of Chemical Innovation Program via the Center for Aerosol Impacts on Climate and the Environment under grant CHE-1305427. Tian Gao is supported by CSC joint PHD project by China Scholarship Council (201606270070). We thank Dr. Zhiguo Li for his efforts in initiating this project. We thank Jiaxi Wang for help fabricating surface patterns and setting up Gaussian calculations. We also appreciate the generous help from John Trueblood and Dr. Vicki Grassian. Lithographic pattern and optical imaging were done in part at San Diego Nanotechnology Infrastructure (SDNI) of UCSD, an NSF-designated National Nanotechnology Coordinated Infrastructure site, which is supported by NSF grant ECCS-1542148).

REFERENCES

(1) Fang, M.; Baldelli, S. Grain Structures and Boundaries on Microcrystalline Copper Covered with an Octadecanethiol Monolayer Revealed by Sum Frequency Generation Microscopy. *J. Phys. Chem. Lett.* **2015**, *6*, 1454–1460.

(2) Fang, M.; Baldelli, S. Surface-Induced Heterogeneity Analysis of an Alkanethiol Monolayer on Microcrystalline Copper Surface Using Sum Frequency Generation Imaging Microscopy. *J. Phys. Chem. C* **2017**, *121*, 1591–1601.

(3) Bredenbeck, J.; Ghosh, A.; Nienhuys, H.-K.; Bonn, M. Interface-Specific Ultrafast Two-Dimensional Vibrational Spectroscopy. *Acc. Chem. Res.* **2009**, *42*, 1332–1342.

(4) Humbert, B.; Grausem, J.; Burneau, A.; Spajer, M.; Tadjeddine, A. Step towards Sum Frequency Generation Spectromicroscopy at a Submicronic Spatial Resolution. *Appl. Phys. Lett.* **2001**, *78*, 135–137.

(5) Raghunathan, V.; Han, Y.; Korth, O.; Ge, N.-H.; Potma, E. O. Rapid Vibrational Imaging with Sum Frequency Generation Microscopy. *Opt. Lett.* **2011**, *36*, 3891.

(6) Shen, Y.; Swiatkiewicz, J.; Winiarz, J.; Markowicz, P.; Prasad, P. N. Second-Harmonic and Sum-Frequency Imaging of Organic Nanocrystals with Photon Scanning Tunneling Microscope. *Appl. Phys. Lett.* **2000**, *77*, 2946–2948.

(7) Ji, N.; Zhang, K.; Yang, H.; Shen, Y. R. Three-Dimensional Chiral Imaging by Sum-Frequency Generation. *J. Am. Chem. Soc.* **2006**, *128*, 3482–3483.

(8) Schaller, R. D.; Saykally, R. J. Near-Field Infrared Sum-Frequency Generation Imaging of Chemical Vapor Deposited Zinc Selenide. *Langmuir* **2001**, *17*, 2055–2058.

(9) Cimatu, K.; Baldelli, S. Sum Frequency Generation Microscopy of Microcontact-Printed Mixed Self-Assembled Monolayers. *J. Phys. Chem. B* **2006**, *110*, 1807–1813.

(10) Lee, C. M.; Kafle, K.; Huang, S.; Kim, S. H. Multimodal Broadband Vibrational Sum Frequency Generation (MM-BB-V-SFG) Spectrometer and Microscope. *J. Phys. Chem. B* **2016**, *120*, 102–116.

(11) Flörsheimer, M.; Brillert, C.; Fuchs, H. Chemical Imaging of Interfaces by Sum Frequency Microscopy. *Langmuir* **1999**, *15*, 5437–5439.

(12) Hoffmann, D. M. P.; Kuhnke, K.; Kern, K. Sum-Frequency Generation Microscope for Opaque and Reflecting Samples. *Rev. Sci. Instrum.* **2002**, *73*, 3221–3226.

(13) Alayoglu, S.; Krier, J. M.; Michalak, W. D.; Zhu, Z.; Gross, E.; Somorjai, G. A. In Situ Surface and Reaction Probe Studies with Model Nanoparticle Catalysts. *ACS Catal.* **2012**, *2*, 2250–2258.

(14) Nguyen, K. T.; King, J. T.; Chen, Z. Orientation Determination of Interfacial β-Sheet Structures in Situ. *J. Phys. Chem. B* **2010**, *114*, 8291–8300.

(15) Ju, L.; Geng, B.; Horng, J.; Girit, C.; Martin, M.; Hao, Z.; Bechtel, H. a; Liang, X.; Zettl, A.; Shen, Y. R.; Wang, F. Graphene Plasmonics for Tunable Terahertz Metamaterials. *Nat. Nanotechnol.* **2011**, *6*, 630–634.

(16) Shopsowitz, K. E.; Qi, H.; Hamad, W. Y.; Maclachlan, M. J. Free-Standing Mesoporous Silica Films with Tunable Chiral Nematic Structures. *Nature* **2010**, *468*, 422–425.

(17) Baiz, C. R.; Schach, D.; Tokmakoff, A. Ultrafast 2D IR Microscopy. *Opt. Express* **2014**, *22* (15), 18724.

(18) Ostrander, J. S.; Serrano, A. L.; Ghosh, A.; Zanni, M. T. Spatially Resolved Two-Dimensional Infrared Spectroscopy via Wide-Field Microscopy. *ACS Photonics* **2016**, *3*, 1315–1323.

(19) Guo, Z.; Wan, Y.; Yang, M.; Snaider, J.; Zhu, K.; Huang, L. Long-Range Hot-Carrier Transport in Hybrid Perovskites Visualized by Ultrafast Microscopy. *Science* **2017**, *356* , 59–62.

(20) Gabriel, M. M.; Kirschbrown, J. R.; Christesen, J. D.; Pinion, C. W.; Zigler, D. F.; Grumstrup, E. M.; Mehl, B. P.; Cating, E. E. M.; Cahoon, J. F.; Papanikolas, J. M. Direct Imaging of Free Carrier and Trap Carrier Motion in Silicon Nanowires by Spatially-Separated Femtosecond Pump–Probe Microscopy. *Nano Lett.* **2013**, *13*, 1336–1340.

(21) Wong, C. Y.; Penwell, S. B.; Cotts, B. L.; Noriega, R.; Wu, H.; Ginsberg, N. S. Revealing Exciton Dynamics in a Small-Molecule Organic Semiconducting Film with Subdomain Transient Absorption Microscopy. *J. Phys. Chem. C* **2013**, *117*, 22111–22122.

(22) Freund, I.; Deutsch, M. Second-Harmonic Microscopy of Biological Tissue. *Opt. Lett.* **1986**, *11* , 94–96.

(23) Shen, Y. R. Phase-Sensitive Sum-Frequency Spectroscopy. *Annu. Rev. Phys. Chem.* **2013**, *64*, 129–150.

(24) Nihonyanagi, S.; Mondal, J. A.; Yamaguchi, S.; Tahara, T. Structure and Dynamics of Interfacial Water Studied by Heterodyne-Detected Vibrational Sum-Frequency Generation. *Annu. Rev. Phys. Chem.* **2013**, *64*, 579–603.

(25) Wang, H.-F.; Velarde, L.; Gan, W.; Fu, L. Quantitative Sum-Frequency Generation Vibrational Spectroscopy of Molecular Surfaces and Interfaces: Lineshape, Polarization, and Orientation SFG-VS: Sum-Frequency Generation Vibrational Spectroscopy. *Annu. Rev. Phys. Chem* **2015**, *66*, 189–216.

(26) Ahmed, M.; Namboodiri, V.; Mathi, P.; Singh, A. K.; Mondal, J. A. How Osmolyte and Denaturant Affect Water at the Air-Water Interface and in Bulk: A Heterodyne-Detected Vibrational Sum Frequency Generation (HD-VSFG) and Hydration Shell Spectroscopic Study. *J. Phys. Chem. C* **2016**, *120*, 10252–10260.

(27) Vanselous, H.; Petersen, P. B. Extending the Capabilities of Heterodyne-Detected Sum-Frequency Generation Spectroscopy: Probing Any Interface in Any Polarization Combination. *J. Phys. Chem. C* **2016**, *120*, 8175–8184.

(28) Okuno, M.; Ishibashi, T. A. Heterodyne-Detected Achiral and Chiral Vibrational Sum Frequency Generation of Proteins at Air/water Interface. *J. Phys. Chem. C* **2015**, *119* , 9947–9954.

(29) Tian, C. S.; Shen, Y. R. Isotopic Dilution Study of the Water/vapor Interface by Phase-Sensitivesum-Frequency Vibrational Spectroscopy. *J. Am. Chem. Soc.* **2009**, *131*, 2790–2791.

(30) Ostroverkhov, V.; Waychunas, G. A.; Shen, Y. R. New Information on Water Interfacial Structure Revealed by Phase-Sensitive Surface Spectroscopy. *Phys. Rev. Lett.* **2005**, *94*, 2–5.

(31) Rich, C. C.; Mattson, M. A.; Krummel, A. T. Direct Measurement of the Absolute Orientation of N3 Dye at Gold and Titanium Dioxide Surfaces with Heterodyne-Detected Vibrational SFG Spectroscopy. *J. Phys. Chem. C* **2016**, *120*, 6601–6611.

(32) Xiong, W.; Laaser, J. E.; Mehlenbacher, R. D.; Zanni, M. T. SI Adding a Dimension to the Infrared Spectra of Interfaces Using Heterodyne Detected 2D Sum-Frequency Generation (HD 2D SFG) Spectroscopy. *Proc. Natl. Acad. Sci.* **2011**, *108*, 20902–20907.

(33) Nihonyanagi, S.; Yamaguchi, S.; Tahara, T. Direct Evidence for Orientational Flip-Flop of Water Molecules at Charged Interfaces: A Heterodyne-Detected Vibrational Sum Frequency Generation Study. *J. Chem. Phys.* **2009**, *130*, 204704.

(34) Chen, X.; Hua, W.; Huang, Z.; Allen, H. C. Interfacial Water Structure Associated with Phospholipid Membranes Studied by Phase-Sensitive Vibrational Sum Frequency Generation Spectroscopy. *J. Am. Chem. Soc.* **2010**, *132*, 11336–11342.

(35) Xu, B.; Wu, Y.; Sun, D.; Dai, H.-L.; Rao, Y. Stabilized Phase Detection of Heterodyne Sum Frequency Generation for Interfacial Studies. *Opt. Lett.* **2015**, *40*, 4472–4475.

(36) Stiopkin, I. V.; Jayathilake, H. D.; Bordenyuk, A. N.; Benderskii, A. V. Heterodyne-Detected Vibrational Sum Frequency Generation Spectroscopy. *J. Am. Chem. Soc.* **2008**, *130*, 2271–2275.

(37) Xiong, W.; Strasfeld, D. B.; Shim, S. H.; Zanni, M. T. Automated 2D IR Spectrometer Mitigates the Influence of High Optical Densities. *Vib. Spectrosc.* **2009**, *50*, 136–142.

(38) Gallagher, S. M.; Albrecht, A. W.; Hybl, J. D.; Landin, B. L.; Rajaram, B.; Jonas, D. M. Heterodyne Detection of the Complete Electric Field of Femtosecond Four-Wave Mixing Signals. *J. Opt. Soc. Am. B* **1998**, *15*, 2338.

(39) Covert, P. A.; FitzGerald, W. R.; Hore, D. K. Simultaneous Measurement of Magnitude and Phase in Interferometric Sum-Frequency Vibrational Spectroscopy. *J. Chem. Phys.* **2012**, *137*, 14201.

(40) Han, Y.; Raghunathan, V.; Feng, R.; Maekawa, H.; Chung, C.-Y.; Feng, Y.; Potma, E. O.; Ge, N.-H. Mapping Molecular Orientation with Phase Sensitive Vibrationally Resonant Sum-Frequency Generation Microscopy. *J. Phys. Chem. B* **2013**, *117*, 6149–6156.

(41) Denk, W.; Strickler, J.; Webb, W. Two-Photon Laser Scanning Fluorescence Microscopy. *Science (80-.).* **1990**, *248*, 73–76.

(42) Jiang, L.; Peng, Y.; Yan, Y.; Deng, M.; Wang, Y.; Huang, J. “Annular Ring” Microtubes Formed by SDS@2β-CD Complexes in Aqueous Solution. *Soft Matter* **2010**, *6*, 1731–1736.

(43) Fu, L.; Wang, Z.; Psciuk, B. T.; Xiao, D.; Batista, V. S.; Yan, E. C. Y. Characterization of Parallel β-Sheets at Interfaces by Chiral Sum Frequency Generation Spectroscopy. *J. Phys. Chem. Lett.* **2015**, *6*, 1310–1315.

(44) Buchbinder, A. M.; Weitz, E.; Geiger, F. M. When the Solute Becomes the Solvent: Orientation, Ordering, and Structure of Binary Mixtures of 1-Hexanol and Cyclohexane over the (0001) α-Al_2O_3 Surface. *J. Am. Chem. Soc.* **2010**, *132*, 14661–14668.

(45) Curtis, A. D.; Reynolds, S. B.; Calchera, A. R.; Patterson, J. E. Understanding the Role of Nonresonant Sum-Frequency Generation from Polystyrene Thin Films. *J. Phys. Chem. Lett.* **2010**, *1*, 2435–2439.

(46) Liu, A. A.; Liu, S.; Zhang, R.; Ren, Z. Spectral Identification of Methanol on TiO_2(110) Surfaces with Sum Frequency Generation in the C-H Stretching Region. *J. Phys. Chem. C* **2015**, *119*, 23486–23494.

(47) Laaser, J. E.; Xiong, W.; Zanni, M. T. Time-Domain SFG Spectroscopy Using Mid-IR Pulse Shaping: Practical and Intrinsic Advantages. *J. Phys. Chem. B* **2011**, *115*, 2536–2546.

(48) Lee, E. *Raman Imaging*; Zoubir, A., Ed.; Springer Series in Optical Sciences; Springer Berlin Heidelberg: Berlin, Heidelberg, 2012; Vol. 168.

(49) Jiang, L.; de Folter, J. W. J.; Huang, J.; Philipse, A. P.; Kegel, W. K.; Petukhov, A. V. Helical Colloidal Sphere Structures through Thermo-Reversible Co-Assembly with Molecular Microtubes. *Angew. Chemie Int. Ed.* **2013**, *52*, 3364–3368.

(50) Brocos, P.; Díaz-Vergara, N.; Banquy, X.; Pérez-Casas, S.; Costas, M.; Piñeiro, A. Similarities and Differences Between Cyclodextrin−Sodium Dodecyl Sulfate Host−Guest Complexes of Different Stoichiometries: Molecular Dynamics Simulations at Several Temperatures. *J. Phys. Chem. B* **2010**, *114*, 12455–12467.

(51) Lee, C. M.; Chen, X.; Weiss, P. A.; Jensen, L.; Kim, S. H. Quantum Mechanical Calculations of Vibrational Sum-Frequency-Generation (SFG) Spectra of Cellulose: Dependence of the CH and OH Peak Intensity on the Polarity of Cellulose Chains within the SFG Coherence Domain. *J. Phys. Chem. Lett.* **2017**, *8*, 55–60.

(52) Vazirani, U.; Papadimitriou, C.; Dasgupta, S. *Algorithms*; McGraw-Hill Education, 2006.

(53) Tyrode, E.; Hedberg, J. A Comparative Study of the CD and CH Stretching Spectral Regions of Typical Surfactants Systems Using VSFS: Orientation Analysis of the Terminal CH_3 and CD_3 Groups. *J. Phys. Chem. C* **2012**, *116* , 1080–1091.

(54) Kouyama, W.; Nishida, T.; Thu Hien, K. T.; Mizutani, G.; Hasegawa, H.; Miyamura, H. Optical Sum Frequency Generation Spectroscopy of Cracked Non-Glutinous Rice (<i>Oryza Sativa</i> L.) Kernels. *J. Biomater. Nanobiotechnol.* **2016**, *7*, 13–18.

(55) Gaussian 16, Revision A.03, M. J. Frisch, G. W. Trucks, H. B. Schlegel, G. E. Scuseria, M. A. Robb, J. R. Cheeseman, G. Scalmani, V. Barone, G. A. Petersson, H. Nakatsuji, X. Li, M. Caricato, A. V. Marenich, J. Bloino, B. G. Janesko, R. Gomperts, B. Mennu, W. C. Gaussian 16. *Gaussian, Inc. Wallingford CT,* **2016**.

(56) Stachowicz, A.; Styrcz, A.; Korchowiec, J.; Modaressi, A.; Rogalski, M. DFT Studies of Cation Binding by β-Cyclodextrin. *Theor. Chem. Acc.* **2011**, *130*, 939–953.

(57) Tang, C. Y.; Huang, Z.; Allen, H. C. Interfacial Water Structure and Effects of Mg^{2+} and Ca^{2+} Binding to the COOH Headgroup of a Palmitic Acid Monolayer Studied by Sum Frequency Spectroscopy. *J. Phys. Chem. B* **2011**, *115*, 34–40.

(58) Ebben, C. J.; Ault, A. P.; Ruppel, M. J.; Ryder, O. S.; Bertram, T. H.; Grassian, V. H.; Prather, K. A.; Geiger, F. M. Size-Resolved Sea Spray Aerosol Particles Studied by Vibrational Sum Frequency Generation. *J. Phys. Chem. A* **2013**, *117*, 6589–6601.

(59) Ai, X.; Beard, M. C.; Knutsen, K. P.; Shaheen, S. E.; Rumbles, G.; Ellingson, R. J. Photoinduced Charge Carrier Generation in a Poly(3-Hexylthiophene) and Methanofullerene Bulk Heterojunction Investigated by Time-Resolved Terahertz Spectroscopy. *J. Phys. Chem. B* **2006**, *110*, 25462–25471.

(60) Zheng, D.; Lu, L.; Li, Y.; Kelly, K. F.; Baldelli, S. Compressive Broad-Band Hyperspectral Sum Frequency Generation Microscopy to Study Functionalized Surfaces. *J. Phys. Chem. Lett.* **2016**, *7*, 1781–1787.

(61) Miles, G. D.; Shedlovsky, L. Minima in Surface Tension–Concentration Curves of Solutions of Sodium Alcohol Sulfates. *J. Phys. Chem.* **1944**, *48*, 57–62.